https://dx.doi.org/10.1016/j.trc.2022.103809

Truck Routing and Platooning Optimization Considering Drivers' Mandatory Breaks

Min Xu[a], Xiaoyuan Yan[a], Yafeng Yin[b]*

[a] *Department of Industrial and Systems Engineering, The Hong Kong Polytechnic University, Hung Hom, Hong Kong*

[b] *Department of Civil and Environmental Engineering, University of Michigan, Ann Arbor, MI 48109, United States of America*

Abstract

Truck platooning has been touted as one of the most promising technologies to improve fuel efficiency thanks to the reduced air drag of the digitally connected truck's slipstream in a trainlike convoy. The benefits of truck platooning lie in the reduced fuel consumption and labor cost, and the enhanced driving experience. However, these benefits cannot be realized without an appropriate routing, scheduling, and platooning plan of trucks subject to practical constraints, especially the drivers' break requirement for long-haul journeys. This study addresses the truck routing and platooning problem considering drivers' mandatory breaks as well as other characteristics such as the state-and-position-dependent fuel-saving rates of platooning, trucks' designated intermediate relays, and platoon size limit. The problem is to route the trucks to their respective destinations on time using the least amount of fuel by maximizing the formations of fuel-saving platoons over entire trips while satisfying the break time requirement of drivers. A mixed-integer linear programming (MILP) model is first developed for the proposed problem. A hybrid algorithm integrating the partial-MILP approach and iterated neighborhood search with tailored search operators is proposed to address the problem. Various randomly generated networks are used in numerical experiments to examine the effectiveness and efficiency of our proposed model and solution method. An extensive sensitivity analysis is also conducted to explore the impacts of several major influential factors, i.e., the drivers' mandatory break times, the fuel reduction rate of the leading truck of platoons, as well as the width of the service time window, on the system performance and derive the managerial insights.

Keywords: truck platooning; mandatory breaks; fuel saving; designated relays; partial-MILP-INS method.

---

* Corresponding author
Tel: +852 2766 6593
Fax: +852 2362 5267
E-mail: xumincee@gmail.com; min.m.xu@polyu.edu.hk (M. Xu)

1. Introduction

The rapid development of connected and autonomous vehicle (CAV) technology will reshape future freight transport services. Touted as the first step towards the implementation of autonomous driving in an open environment, truck platooning, i.e., a convoy of virtually connected trucks driving closely with small headways (see Figure 1), is predicted to become mainstream in the next decade (Bono et al., 2018; Fagnant and Kockelman, 2015). By allowing multiple trucks to drive as one unit, truck platooning could save road space, enhance traffic safety, and notably, offer significant fuel savings and vehicle emission reductions via lowered aerodynamic drag on vehicles (Taylor et al., 2020; Tsugawa et al., 2016; Zhang et al., 2020). Despite these favorable merits, the establishment of platoons requires non-trivial coordination and planning. For example, since the departure times and routes of the trucks in the platoon should be synchronized, a truck may need to wait for other trucks or make a detour to form or join a platoon. For the freight transport services with temporally and spatially distributed delivery requests in particular, how to determine the routes and schedules of the trucks in a fleet that reap the fuel-saving benefits without deteriorating the logistics service quality is one of the most pressing challenges faced by autonomous freight transport service providers.

Figure 1. Illustration of a three-truck platoon (Larsson et al., 2015)

1.1. Literature review

Over the past decades, many studies have been devoted to vehicle/truck platooning concerning the technical issues and impact analysis, such as the design and control of platoons to maintain the desired space and ensure the string stability, the evaluation of platoons in terms of safety, fuel savings, etc. (Goñi-Ros et al., 2019; Li et al., 2017; Mahdinia et al., 2020; Wang et al., 2020, Zheng et al., 2022). Nevertheless, the literature review by Bhoopalam et al. (2018) found that the planning and optimization of truck platooning received insufficient attention.

Among these limited studies, Larson et al. (2013) were the first to maximize the platoon opportunities of trucks with different itineraries. They proposed a distributed method enabled by local controllers at road intersections to adjust the speed of trucks approaching the intersections in anticipation of platooning with others. Later, Larsson et al. (2015) formally introduced a general truck platooning problem (TPP) that aimed to optimize the routes and schedules of a truck fleet in a network to minimize the total fuel cost given the origin and destination of each truck and proved its NP-hardness. They defined a linear fuel cost function with respect to the platoon size (i.e., the number of trucks traveling along an edge as a platoon) to factor in the fuel-saving benefit of truck platooning. However, they only addressed a special case of the general TPP that ignores the time window constraints of the delivery tasks. Later on, many extensions and follow-up studies have been made upon Larsson et al. (2015), such as enhancing the model formulation, developing more computationally efficient algorithms for large-scale problems, addressing a general TPP problem with time window constraints, additionally optimizing the speed (profile) of the trucks, etc. (Abdolmaleki et al., 2021; Larson et al., 2016; Luo et al., 2018; Luo et al., 2021; Luo and Larson, 2021; Nourmohammadzadeh and Hartmann, 2016; Sokolov et al., 2017; Van De Hoef et al., 2015; Van De Hoef et al., 2018). Apart from the classic TPP, there are also many studies for other interesting problems related to truck platooning under different problem settings (Boysen et al., 2018; Larsen et al., 2019; Sun and Yin, 2019; 2021a; 2021b; Xue et al., 2021; Yan et al., 2022; You et al., 2021; Zhang et al., 2017). For example, Sun and Yin (2019; 2021a; 2021b) investigated novel platoon formulation problems and proposed centralized and decentralized benefit-redistribution mechanisms to achieve "behaviorally stable" platooning. Boysen et al. (2018) looked into a truck scheduling problem considering platooning along a single path. Larsen et al. (2019) optimized the platoon formulation at a hub considering random arrivals of trucks. Xue et al. (2021) and You et al. (2020) studied a local container drayage problem under truck platooning mode. Zhang et al. (2017) investigated a freight transport platoon coordination and departure time scheduling problem under travel time uncertainty.

Although fruitful results have been achieved, most existing studies for the general TPP in a network focused on modeling the temporal and spatial coordination of the platoon itself without considering the drivers' mandatory breaks, which are practically relevant and significant, especially for long-haul journeys. Take the United States for example, in compliance with the Hours of Service (HOS) regulations, to reduce accidents caused by driver fatigue, all truck drivers, either on urban road sectors or on highways, are required to follow the break rule that stipulates the minimum amount of mandatory break time that a driver must take during his/her tour (FMCSA, 2011). Therefore, the routes and schedules of trucks should comply with the drivers' break time requirement. Moreover, other than the increased fuel economy, another notable merit of CAV technology is the reduced labor cost as autonomous trucks are expected to drive themselves without onboard human drivers. Nevertheless, there will be a long way to go before fully autonomous trucks become mainstream (Bono, et al., 2018). According to the European Union roadmap for truck platooning, in the transition stage towards full autonomous trucks, only the driver of the leading truck of a platoon should be present; the drivers in the following trucks of a platoon may not need to be attentive or present (ACEA, 2018; Bhoopalam et al., 2021). Hence, the incorporation of the drivers' break time constraints considering the rest time in the following vehicles of platoons in the context of TPP is highly desired. Recently, Stehbeck (2019) has considered drivers' breaks, and it was found that the consideration of these mandatory breaks would negatively affect the fuel-saving benefit of platooning. Unfortunately, the problem in Stehbeck (2019) was formulated under restrictive assumptions that trucks in a platoon should follow a pre-specified sequence and only the following vehicles will benefit from platooning in terms of fuel-saving.

1.2. Objective and contributions

To bridge the above research gap, this study investigates the truck routing and platooning optimization problem considering the drivers' mandatory breaks for the long-haul freight transportation, referred to as TRP problem thereafter. Drivers are required to take compulsory breaks of certain durations for safe driving over long journeys. We assume that the fuel reduction rates of trucks vary with their states (i.e., as a platoon or traveling alone) and positions (i.e., in the leading or the following positions if platooned). Trucks are allowed to detour and wait at some intersections for platooning opportunities. We also consider intermediate truck relays, e.g., for trucks' maintenance checks, freight pick-ups or deliveries, etc., and assume that the trucks should visit intermediate relay nodes and stay for a certain period of time to conduct the aforementioned necessary tasks along with the long-distance travel. Given the itinerary of each truck, i.e., the origin, the destination, the intermediate relay locations and the required relay times, and the service time window of the whole journey, the objective of this study is to determine the optimal route and platoon plan of the truck fleet that minimizes the total fuel cost over the entire trips without violating the constraints for service time window, drivers' mandatory breaks, and trucks' relays.

To achieve the objective, we formulate a novel mixed-integer linear programming (MILP) model that can effectively differentiate the truck traveling alone and that as the leader and follower of a platoon and incorporate the drivers' mandatory breaks, state-and-position-dependent fuel reduction rates, and intermediate relay constraints. Due to the complexity of the problem, the proposed MILP model is computationally challenging even for a small-sized problem, if solved directly by commercial solvers. Therefore, we design a customized hybrid algorithm integrating the partial-MILP approach and iterated neighborhood search (INS) by exploring the features of the TRP problem to obtain good-quality solutions. Numerical experiments are conducted to demonstrate the efficacy of the proposed model and algorithm as well as to examine the impacts of several influential factors on platooning-related performance and derive managerial insights for relevant stakeholders.

The remainder of this study is organized as follows. Assumptions, notations, and problem description are elaborated in Section 2, followed by the formulation of a MILP model for TRP problem in Section 3. Section 4 describes the partial-MILP optimization algorithm with tailor-made neighbourhood search operators. The efficiency of the proposed model and algorithm and the impacts of three influential factors on the system performance are evaluated in Section 5. Section 6 presents the conclusions and future research directions.

2. Assumptions, notations, and problem description

We define the TRP problem over a directly highway network $\mathbf{G}=(\mathbf{N},\mathbf{E})$, where $\mathbf{N}$ is the node set and $\mathbf{E}$ is the edge set. Each edge $(i,j)\in\mathbf{E}$, $\forall i,j\in\mathbf{N}$ corresponds to a road segment in the highway network, while each node $i\in\mathbf{N}$ represents the intersection of the network. Let $\mathbf{V}$ be the set of involved trucks, which are homogenous with respect to vehicle specification and configuration. Each truck $v\in\mathbf{V}$ has an itinerary characterized by the origin node $o_v\in\mathbf{N}$, the destination node $d_v\in\mathbf{N}$, the service time window, i.e., the earliest departure time σ_v from the origin node $o_v\in\mathbf{N}$ and the latest arrival time τ_v at the destination node $d_v\in\mathbf{N}$, the intermediate relay nodes grouped in set $\mathbf{N}^v\subseteq\mathbf{N}$, and the required relay time e_i^v at each intermediate relay node $i\in\mathbf{N}^v$. For simplicity, all the involved trucks are assumed to travel at a free-flow speed on each edge $(i,j)\in\mathbf{E}$ in the network and the time required to traverse an edge $(i,j)\in\mathbf{E}$ is denoted by w_{ij}. To fully present the TRP problem of our interest, we will elaborate on the truck platooning, the drivers' mandatory breaks and designated relays, and state-and-position-dependent fuel reduction rate in the following subsections. The notations used throughout this study are provided in the appendix for readability.

2.1. Truck platooning

Regarding truck platooning, we assume that the formulation and dissolution of platoons can only occur at the nodes of the network. Trucks are assumed to form a platoon when they start traversing an edge at the same time, and they will travel together throughout the edge at the constant free-flow speed until the next edge. Trucks are allowed to take detours or wait at some nodes to join or form a platoon as long as the service time windows are respected. For safety concerns, the size of platoons on each edge cannot exceed a pre-specified threshold. To formulate truck platooning that requires both the spatial and temporal synchronization of several trucks, in addition to the binary route variables x_{ij}^{v} , $\forall (i,j)\in \mathbf{E}, v\in \mathbf{V}$ and the continuous time variables t_i^v, $\forall i\in \mathbf{N}, v\in \mathbf{V}$, indicating whether truck v traverses edge (i,j) on its trip and the time instant at which the truck v starts traversing an edge from node i, respectively, we need to define binary platoon variables p_{ij}^{vw}, $\forall\ (i,j)\in \mathbf{E}, v\neq w\in \mathbf{V}$, to denote whether truck v will travel in a position behind truck w in the same platoon over edge (i,j) (Kindly note that trucks v and w may not be adjacent).

Specifically, to form a platoon, trucks v and w should simultaneously traverse the same edge as formulated by

$$2p_{ij}^{vw} \le x_{ij}^{v}+x_{ij}^{w}, \quad \forall (i,j)\in \mathbf{E}, v\neq w\in \mathbf{V} \tag{1}$$

$$-M_1^{vw}(1-p_{ij}^{vw}) \le t_i^v - t_i^w \le M_1^{vw}(1-p_{ij}^{vw}), \quad \forall (i,j)\in \mathbf{E}, v\neq w\in \mathbf{V} \tag{2}$$

where M_1^{vw} is a sufficiently large number satisfying $M_1^{vw} \ge \min\{\tau_v,\tau_w\} - \max\{\sigma_v,\sigma_w\}$. Eq. (1) imposes that trucks v and w will not be in a platoon on an edge that is not traversed by both of them. Eq. (2) enforces that trucks v and w should travel from the same node at the same time if they form a platoon at that node. In addition, to further express the relative position relationship between truck v and truck w if they are platooned, we should have the following constraints:

$$p_{ij}^{vw} + p_{ij}^{wv} \le 1, \quad \forall (i,j)\in \mathbf{E}, v\neq w\in \mathbf{V} \tag{3}$$

$$\sum_{k\in \mathbf{V}} p_{ij}^{vk} - \sum_{k\in \mathbf{V}} p_{ij}^{wk} \ge 1 - M_2(1-p_{ij}^{vw}), \quad \forall (i,j)\in \mathbf{E}, v\neq w\in \mathbf{V} \tag{4}$$

where M_2 is a sufficiently large number satisfying $M_2 \ge |\mathbf{V}|$. Eq. (3) guarantees that either truck v travels behind truck w or vice versa, whereas Eq. (4) indicates that truck v is deemed to travel behind truck w in a platoon if the number of trucks traveling ahead of truck v in the platoon is larger than that of truck w. Moreover, to enforce the platoon size limit, the following constraint is required:

$$\sum_{w \in \mathbf{V}} p_{ij}^{vw} + 1 \leq L_{ij}, \quad \forall (i, j) \in \mathbf{E}, v \in \mathbf{V} \tag{5}$$

where L_{ij} is the pre-specified maximum size of a platoon on edge (i, j).

2.2. Drivers' mandatory breaks and intermediate truck relays

With the advance of CAV technology in the foreseeable future, the drivers in the following trucks of a platoon may not need to be attentive or present. Instead, they may rest when traveling behind other truck(s) in a platoon unless some intervention is required to dissolute the platoon or form a new platoon (ACEA, 2018; Bhoopalam et al., 2021). Many countries around the world have implemented drivers break time regulations to prevent driver fatigue and ensure safety. However, the break rules vary greatly and there are several versions or exceptions (Goel and Rousseau, 2012). For instance, in Europe, truck drivers must take at least a 45-minute break when they have continuously driven for 4.5 hours without interruption according to the Regulation (EC) No 561/2006 (Gibraltarlaws, 2021). Another example is that a 30-minute break is required for the truck drivers after 8 cumulative driving hours without a break to abide by the HOS rules in the United States (FMCSA, 2011). In Australia, a driver must take a mandatory 15-min break prior to the completion of 5.5 hours of continuous driving (Abdulahovic and Edlund, 2018). We can find that the drivers' break time regulations vary significantly from one another and these rules may be subject to radical changes along with the development of vehicle automation level. Therefore, in this study, we consider a generic and simplified break rule that the driver's mandatory break time can be distributed over the whole journey and the total break time of the driver of truck v, including the waiting times and relay times of the truck, and notably, the time following some other truck(s) in the form of a platoon, should not be less than a threshold denoted by T_v. Kindly note that the waiting times and relay times at the origin and destination nodes of a truck should be excluded to ensure that the break time is distributed through the route. Besides, truck $v \in \mathbf{V}$ should visit the designated intermediate relay node $i \in \mathbf{N}^v$ and stay there for at least e_i^v to conduct necessary maintenance checks, delivery, and/or pick-up tasks during the long-distance journey.

To model the above practical constraints, we define binary decision variables β_{ij}^{v}, $\forall(i,j)\in\mathbf{E}, v\in\mathbf{V}$, indicating whether truck v trails behind some truck(s) in a platoon when traversing edge (i,j), and continuous decision variables u_i^v, $\forall i\in\mathbf{N}, v\in\mathbf{V}$, denoting the dwell time of truck $v\in\mathbf{V}$ at node $i\in\mathbf{N}$. Kindly note that a truck may dwell at node $i\in\mathbf{N}$ waiting to join or form a platoon, for a break, for a necessary relay, or all of them. It is straightforward that we have the following relationship between the route variables x_{ij}^{v} and the platoon variables β_{ij}^{v}:

$$\beta_{ij}^{v} \le x_{ij}^{v}, \quad \forall(i,j)\in\mathbf{E}, v\in\mathbf{V} \tag{6}$$

which suggests that it is impossible for a truck to be a follower of a platoon on an edge that is not traversed by that truck. We then proceed to establish the relationship between p_{ij}^{vw} and β_{ij}^{v}. Particularly, for a specific truck v traveling along edge (i,j), let A_{ij}^{v} denote the number of trucks traveling ahead of truck v in the same platoon along edge (i,j) that is given by

$$A_{ij}^{v} = \sum_{w\in\mathbf{V}, w\neq v} p_{ij}^{vw}, \quad \forall(i,j)\in\mathbf{E}, v\in\mathbf{V} \tag{7}$$

It can be readily seen that β_{ij}^{v} is determined by A_{ij}^{v} as follows:

$$\beta_{ij}^{v} = \begin{cases} 1, & \text{if } A_{ij}^{v} \ge 1 \\ 0, & \text{if } A_{ij}^{v} = 0 \end{cases}, \quad \forall(i,j)\in\mathbf{E}, v\in\mathbf{V} \tag{8}$$

The above equation shows that the value of β_{ij}^{v} depends on A_{ij}^{v} only. Considering that β_{ij}^{v} is a binary variable, the relationship between β_{ij}^{v} and A_{ij}^{v} in Eq. (8) can be equivalently expressed by the following constraint:

$$\frac{A_{ij}^{v}}{M_3} \le \beta_{ij}^{v} \le A_{ij}^{v}, \quad \forall(i,j)\in\mathbf{E}, v\in\mathbf{V} \tag{9}$$

where M_3 is a sufficiently large number satisfying $M_3 \ge |\mathbf{V}|-1$.

Given the decision variables β_{ij}^{v} and u_i^v, the total break time of the driver of truck v can thus be calculated by $\sum_{i\in\mathbf{N}\backslash\{o_v,d_v\}} u_i^v + \sum_{(i,j)\in\mathbf{E}} w_{ij}\beta_{ij}^{v}$. Hence, for the drivers' mandatory breaks, we have the following constraint:

$$\sum_{i \in \mathbf{N} \setminus \{o_v, d_v\}} u_i^v + \sum_{(i,j) \in \mathbf{E}} w_{ij} \beta_{ij}^v \geq T_v, \quad \forall v \in \mathbf{V} \tag{10}$$

in which the threshold T_v can be set to be a pre-determined value based on the shortest travel time from the origin to the destination of truck v or a percentage of the actual duration of the journey given by $(t_{d_v}^v - u_{d_v}^v - t_{o_v}^v)$. For the designated relays of trucks, it requires that

$$\sum_{\{j|(i,j) \in \mathbf{E}\}} x_{ij}^v = 1, \quad \forall i \in \mathbf{N}^v, v \in \mathbf{V} \tag{11}$$

$$u_i^v \geq e_i^v, \quad \forall i \in \mathbf{N}^v, v \in \mathbf{V} \tag{12}$$

where Eqs. (11) and (12) ensure that truck $v \in \mathbf{V}$ traverses all the relay nodes and the dwell time at each relay node is not less than the stipulated duration, respectively.

2.3. State-and-position-dependent fuel reduction rate

For the fuel cost, many field experiments and simulation studies have revealed that when traveling as a platoon, not only the following trucks but also the leader will experience significant fuel reduction (Davila et al., 2013; Lammert et al., 2014; Lu and Shladover, 2014). To align with the findings of the literature, we assume that trucks will experience fuel savings when traveling in the form of platoons and the fuel consumption depends on both the state of trucks, i.e., in a platoon or traveling alone, and their positions in a platoon, i.e., in the leading or the following positions. Specifically, taking a truck that drives on its own and experiences no fuel savings as the benchmark, the fuel reduction rates of the leading and following trucks in a platoon, denoted by η_l and η_f, respectively, are assumed to be positive. Let c_{ij} denote the fuel cost of a truck on edge (i, j) if it travels alone; then the fuel cost of a truck would be $\eta_l c_{ij}$ and $\eta_f c_{ij}$ if it leads a platoon and trails behind other trucks in a platoon along edge (i, j), respectively.

To incorporate the state-and-position-dependent fuel reduction rates of trucks, in addition to the platoon variables β_{ij}^v, we need to define another type of platoon variables, i.e., the binary decision variables λ_{ij}^v, $\forall\ (i, j) \in \mathbf{E}, v \in \mathbf{V}$, denoting whether truck v leads a platoon when traveling across edge (i, j). This variable is introduced to differentiate the truck traveling alone and that as the leader of a platoon so as to facilitate the formulation of fuel saving of the leading trucks. Similar to Eq. (6), we can readily obtain the following relationship between the route variables x_{ij}^v and the platoon variables λ_{ij}^v:

$$\lambda_{ij}^{v} \le x_{ij}^{v}, \quad \forall (i,j) \in \mathbf{E}, v \in \mathbf{V} \tag{13}$$

which limits that it is impossible for a truck to be the leader of a platoon on an edge that is not traversed by that truck. Next, we need further to establish the relationship between p_{ij}^{vw} and λ_{ij}^{v}. For a specific truck v traveling along edge (i,j), its state and position, i.e., whether it travels alone or leads a platoon, not only depend on the number of vehicles traveling in front of it, i.e., A_{ij}^{v}, but also that of vehicles behind it in the same platoon[1] calculated by

$$B_{ij}^{v} = \sum_{w \in \mathbf{V}, w \ne v} p_{ij}^{wv}, \quad \forall (i,j) \in \mathbf{E}, v \in \mathbf{V} \tag{14}$$

where B_{ij}^{v} denotes the number of trucks traveling behind truck v in the same platoon along edge (i,j). Then we have the following information of λ_{ij}^{v} :

$$\lambda_{ij}^{v} = \begin{cases} 1, & \text{if } A_{ij}^{v} = 0, B_{ij}^{v} \ge 1 \\ 0, & \text{if } A_{ij}^{v} \ge 1, B_{ij}^{v} \ge 1 \\ 0, & \text{if } A_{ij}^{v} \ge 1, B_{ij}^{v} = 0 \\ 0, & \text{if } A_{ij}^{v} = 0, B_{ij}^{v} = 0 \end{cases}, \quad \forall (i,j) \in \mathbf{E}, v \in \mathbf{V} \tag{15}$$

Unlike β_{ij}^{v} in Eq. (8) that is determined by A_{ij}^{v} only, the equivalent constraint for the relationships in Eq. (15) cannot be readily derived because the value of λ_{ij}^{v} is jointly determined by A_{ij}^{v} and B_{ij}^{v}. By consolidating the conditions in Eq. (15), we can find that λ_{ij}^{v} would be 0 if either $B_{ij}^{v} = 0$ or $A_{ij}^{v} \ge 1$. For $B_{ij}^{v} = 0$, we have the following constraint to enforce the relationships in the last two sub-equations in Eq. (15) without violating the other relationships in Eq. (15) because Eq. (16) will be a null constraint when $B_{ij}^{v} \ge 1$:

$$\lambda_{ij}^{v} \le B_{ij}^{v}, \quad \forall (i,j) \in \mathbf{E}, v \in \mathbf{V} \tag{16}$$

As for the case of $A_{ij}^{v} \ge 1$, to force λ_{ij}^{v} to be 0, we have two alternative constraints as follows:

$$\lambda_{ij}^{v} \le \frac{A_{ij}^{v}}{M_3}, \quad \forall (i,j) \in \mathbf{E}, v \in \mathbf{V} \tag{17}$$

[1] Kindly note that in terms of configuration, a truck traveling alone can be viewed as a special platoon composed of one vehicle only.

$$\lambda_{ij}^v \le 1 - \frac{A_{ij}^v}{M_3}, \quad \forall (i,j) \in \mathbf{E}, v \in \mathbf{V} \tag{18}$$

It can be seen that either of the above two constraints will restrict λ_{ij}^v to be 0 if $A_{ij}^v \ge 1$, but Eq. (17) will unfavorably make λ_{ij}^v be 0 when $A_{ij}^v = 0$, which contradicts the first sub-equation in Eq. (15). Therefore, only Eq. (18) is applicable because it will reduce to a null constraint when the condition $A_{ij}^v \ge 1$ is not satisfied. We can find that all the relationships in Eq. (15) have been delineated by Constraints (16) and (18) except the first sub-equation since λ_{ij}^v could still be 0 when $A_{ij}^v = 0$ and $B_{ij}^v \ge 1$. To further express the relationship the first sub-equation only when the corresponding condition is satisfied, we shall have an additional constraint to restrict the lower bound of λ_{ij}^v to be larger than 0, i.e.,

$$\lambda_{ij}^v \ge f(A_{ij}^v, B_{ij}^v), \quad \forall (i,j) \in \mathbf{E}, v \in \mathbf{V} \tag{19}$$

where $f(A_{ij}^v, B_{ij}^v)$ had better to be a linear function with respect to A_{ij}^v and/or B_{ij}^v with its value falling between 0 and 1 only when $A_{ij}^v = 0$ and $B_{ij}^v \ge 1$. There are many linear functions, among which the simplest one is $\frac{B_{ij}^v}{M_3}$. However, if $f(A_{ij}^v, B_{ij}^v)$ is set to be $\frac{B_{ij}^v}{M_3}$, Constraint (19) will not be a null constraint for the second sub-equation of Eq. (15). As such, we need an additional term $-A_{ij}^v$ to 'dip' the lower bound for the second sub-equation without affecting the feasible range of the lower bound for the first sub-equation. In other words, we have

$$f(A_{ij}^v, B_{ij}^v) := \frac{B_{ij}^v}{M_3} - A_{ij}^v, \quad \forall (i,j) \in \mathbf{E}, v \in \mathbf{V} \tag{20}$$

It can be easily verified that Eq. (15) can be equivalently expressed by Eqs. (16) and (18)-(20) jointly.

The objective of the TRP problem in this study is to minimize the collective fuel costs of a fleet of trucks by optimizing their itineraries, i.e., the traveling routes, the schedules, and the platoon plans, such that (i) the trucks complete the trips within their service time windows, i.e., arrive at their destinations before the corresponding deadlines; (ii) the drivers take sufficient breaks during the entire journeys; and (iii) the trucks visit the designated relay nodes and complete the intermediate tasks.

3. Optimization model building

With the aforementioned notations, the TRP problem investigated in this study can be formulated by the following model:

[TRP]

$$\min_{\mathbf{x},\mathbf{p},\boldsymbol{\beta},\boldsymbol{\lambda},\mathbf{t},\mathbf{u}} \sum_{v\in\mathbf{V}} \sum_{(i,j)\in\mathbf{E}} c_{ij}\left(x_{ij}^{v} - \eta_f \beta_{ij}^{v} - \eta_l \lambda_{ij}^{v}\right) \tag{21}$$

subject to Eqs. (1)-(7), (9)-(14), (16), (18)-(20), and

$$\sum_{\{j|(i,j)\in\mathbf{E}\}} x_{ij}^{v} - \sum_{\{j|(j,i)\in\mathbf{E}\}} x_{ji}^{v} = \begin{cases} 1, & \text{if } i = o_v \\ -1, & \text{if } i = d_v \\ 0, & \text{otherwise} \end{cases}, \quad \forall i\in\mathbf{N}, v\in\mathbf{V} \tag{22}$$

$$t_j^v \geq t_i^v + w_{ij} + u_j^v - M_4^{ijv}(1 - x_{ij}^v), \quad \forall j\in\mathbf{N}, (i,j)\in\mathbf{E}, v\in\mathbf{V} \tag{23}$$

$$t_{o_v}^v \geq \sigma_v, \quad \forall v\in\mathbf{V} \tag{24}$$

$$t_{d_v}^v \leq \tau_v, \quad \forall v\in\mathbf{V} \tag{25}$$

$$t_i^v \leq M_5^{iv} \sum_{\{j|(i,j)\in\mathbf{E}\}} (x_{ij}^v + x_{ji}^v), \quad \forall i\in\mathbf{N}, v\in\mathbf{V} \tag{26}$$

$$u_i^v \leq M_6^{iv} \sum_{\{j|(i,j)\in\mathbf{E}\}} (x_{ij}^v + x_{ji}^v), \quad \forall i\in\mathbf{N}, v\in\mathbf{V} \tag{27}$$

$$x_{ij}^v, \beta_{ij}^v, \lambda_{ij}^v, p_{ij}^{vw} \in \{0,1\}, \quad \forall (i,j)\in\mathbf{E}, v, w\in\mathbf{V} \tag{28}$$

$$t_{ij}^v \geq 0, u_i^v \geq 0, \quad \forall (i,j)\in\mathbf{E}, v\in\mathbf{V} \tag{29}$$

where M_4^{ijv}, M_5^{iv}, and M_6^{iv} are sufficiently large numbers satisfying $M_4^{ijv} \geq \tau_v + w_{ij}$, $M_5^{iv} \geq \tau_v - \chi_{id_v}$, and $M_6^{iv} \geq (\tau_v - \sigma_v) - \left(\chi_{o_v d_v} + \sum_{j\in\mathbf{N}^v\setminus\{i\}} e_j^v\right)$, respectively, in which χ_{ij} denotes the travel time of the shortest path from node $i\in\mathbf{N}$ to node $j\in\mathbf{N}$.

The objective function in Eq. (21) is the sum of the fuel costs incurring on all edges traversed by the whole fleet considering different fuel-saving rates of trucks in different states and positions. Constraints (1)-(7), (9)-(14), (16), and (18)-(20) have been elaborated in Section 2. Constraint (22) ensures the flow conservation for each truck. Eqs. (23)-(25) are the constraints for the truck schedules. Specifically, Constraint (23) updates the time instant each truck starts traveling along the edge from a node. If $x_{ij}^v = 1$, it reduces to $t_j^v \geq t_i^v + w_{ij} + u_j^v$, which requires the truck to depart from node j at a time not earlier than the departure time from node i plus the travel time over edge (i, j) and the dwell time at node j; and becomes redundant, otherwise. Constraints (24) and (25) impose the service time window constraint. Constraints (26) and (27) restrict the departure time instant and the dwell time at nodes that are not visited by the trucks to be 0, respectively. Constraints (28) and (29) define the domains of the decision variables.

4. Solution method design

The model [TRP] formulated in Section 3 is a MILP model, which can be solved directly by commercial solvers like CPLEX. However, our preliminary experiments have found that the solver CPLEX fails to solve even a small instance with 8 trucks in a highway network with 10 nodes within 1 hr. This could be attributed to the complex model structure and a large number of variables in the model [TRP]. Therefore, in this section, we propose a customized hybrid algorithm named the partial-MILP method with iterated neighborhood search (P-MILP-INS) to address the problem.

The P-MILP-INS is a hybrid algorithm integrating the partial-MILP method and iterated neighborhood search (INS). It has been used by Xiao and Konak (2016) for large-sized heterogeneous green vehicle routing and scheduling problem. Following the framework of INS, given an initial solution, the proposed method will employ an efficient partial-MILP method to generate better solutions in the neighborhoods of the incumbent solution in each search iteration. As indicated by the name 'partial-MILP', a better solution will be obtained by solving a partial MILP model with some variables fixed to be the values of the incumbent solution. In this way, only a subset of variables, referred to as unfixed variables, remain to be optimized and thus the computation time will be reduced. The efficacy of P-MILP-INS depends on whether we can identify an appropriate subset of variables, the re-optimization of which could efficiently and effectively improve the incumbent solution. In what follows, we will elaborate on the partial-MILP method, especially the way to select the set of unfixed variables for our problem, and the framework of P-MILP-INS in Subsections 4.1 and 4.2, respectively.

4.1. An efficient partial-MILP approach

To apply the partial-MILP method, we will first confirm the types of variables that contribute much the computational challenge to the model [TRP] and/or that are crucial and decisive to the objective function value of the model. On the one hand, fixing a subset of these types of variables will lead to a great reduction of computation time in each search iteration. On the other hand, the re-optimization of the remaining variables of these types will likely generate a better solution upon the incumbent one. Hence, a good choice for the types of variables will help to achieve high computational efficiency and good solution quality overall. For the considered TRP problem, we have three types of variables, i.e., one route variable x_{ij}^{v}, three platoon variables p_{ij}^{vw}, β_{ij}^{v}, and λ_{ij}^{v}, and two time variables t_{i}^{v} and u_{i}^{v}. Among the three types of variables, the route and platoon variables are good candidates since they appear directly in the objective function (21), and most importantly, once the routing and platooning strategies are known, the time variables for fleet schedules can be determined rather efficiently. Therefore, we will select and fix/unfix a subset of route and platoon variables, i.e., x_{ij}^{v}, p_{ij}^{vw}, β_{ij}^{v}, and λ_{ij}^{v}, when employing the partial-MILP method.

As for the selection of the subset of route and platoon variables, we propose the following five tailor-made neighborhood search operators, i.e., OP-1, OP-2, …, OP-5, to construct the unfixed variables in set $\mathbf{\Omega}$ to be re-optimized:

(i) Random-node-selection (OP-1)

The first operator, referred to as random-node-selection, is to randomly select W_1 nodes among the nodes in the network and all the route and platoon variables associated with these nodes will be put into set $\mathbf{\Omega}$. Let $\mathbf{N}_1 \subseteq \mathbf{N}$ denote the subset of the randomly selected nodes by OP-1; then the set of unfixed variables is denoted by $\mathbf{\Omega} = \{x_{ij}^{v}, p_{ij}^{vw}, \beta_{ij}^{v}, \lambda_{ij}^{v}, \forall i \in \mathbf{N}_1, (i, j) \in \mathbf{E}, v, w \in \mathbf{V}\}$.

(ii) Nearest-node-selection (OP-2)

The second operator, named nearest-node-selection, is to randomly select one node $i \in \mathbf{N}$ and its $(W_2 - 1)$ nearest neighbors in terms of the shortest travel time to node i. Again, all the route and platoon variables associated with these nodes will be put into set $\mathbf{\Omega}$. Let $\mathbf{N}_2 \subseteq \mathbf{N}$ denote the subset of the selected nodes by OP-2; then the set of unfixed variables is denoted by $\mathbf{\Omega} = \{x_{ij}^{v}, p_{ij}^{vw}, \beta_{ij}^{v}, \lambda_{ij}^{v}, \forall i \in \mathbf{N}_2, (i, j) \in \mathbf{E}, v, w \in \mathbf{V}\}$.

(iii) Random-truck-selection (OP-3)

The third operator, called random-truck-selection, is to randomly select a truck among set $\mathbf{V}$ and all the route and platoon variables associated with the truck will be put into set $\mathbf{\Omega}$. Let $\hat{v}$ denote the selected truck index; then the set of unfixed variables is represented by $\mathbf{\Omega} = \{x_{ij}^{\hat{v}}, p_{ij}^{\hat{v}w}, \beta_{ij}^{\hat{v}}, \lambda_{ij}^{\hat{v}}, \forall (i, j) \in \mathbf{E}, w \in \mathbf{V}\}$.

(iv) Nearest-truck-selection (OP-4)

The fourth operator, named nearest-route-selection, is to randomly select a truck and its 'nearest' truck in terms of the composite distance defined by

$$\zeta_{vw} = \sqrt{\chi^2_{o_v o_w} + \chi^2_{d_v d_w} + (\sigma_v - \sigma_w)^2 + (\tau_v - \tau_w)^2}, \quad \forall v, w \in \mathbf{V} \tag{30}$$

where $\chi_{o_v o_w}$ and $\chi_{d_v d_w}$ denote the shortest travel times between the origins and the destinations of the trucks v and w, respectively. It can be seen that the above composite distance measures the degree of the spatial and temporal synchronization of the itineraries, and accordingly the likelihood of platooning, of two trucks. All the route and platoon variables associated with the two trucks will be put into set $\mathbf{\Omega}$. Let $\hat{v}^1$ and $\hat{v}^2$ denote the selected two trucks; then the set of unfixed variables is represented by $\mathbf{\Omega} = \{x_{ij}^{\hat{v}^1}, x_{ij}^{\hat{v}^2}, p_{ij}^{\hat{v}^1 w}, p_{ij}^{\hat{v}^2 w}, \beta_{ij}^{\hat{v}^1}, \beta_{ij}^{\hat{v}^2}, \lambda_{ij}^{\hat{v}^1}, \lambda_{ij}^{\hat{v}^2}, \forall (i, j) \in \mathbf{E}, w \in \mathbf{V}\}$.

(v) Nearest-2-truck-selection (OP-5)

The last operator, named nearest-2-route-selection, is similar to OP-4. The only difference is that OP-5 will select a truck and its two 'nearest' trucks according to Eq. (30). Analogously, all the route and platoon variables associated with the three trucks will be put into set $\mathbf{\Omega}$.

The OP-1 and OP-2 are node-based selection operators. Generally speaking, the larger the number of nodes selected for re-optimization, the more significant the improvement on the incumbent solution could be made at the expense of an increased computational time. As such, the values of W_1 and W_2 should be carefully chosen to strike a good balance between solution quality and computational efficiency in each search iteration. Moreover, different from OP-1 that randomly selects all the nodes, OP-2 focuses on the nodes clustered around a master node, considering that a better routing and platooning plan will not spatially differ too much from the incumbent one. Note that a large detour for platoon opportunities and cost savings could be offset by the increased fuel cost of the detour itself. The other three operators, i.e., OP-3, OP-4, and OP-5, are truck-based selection operators. The OP-3 selects only one truck, and thus the routing and platooning plan of this truck will be re-optimized given the incumbent solution of all the other trucks. The OP-4 and OP-5 extend OP-3 by unfixing the variables related to multiple trucks that share similar itineraries, and thus there is a high chance that these trucks could form (better) platoons through re-optimization. The combination of the five different neighborhood search operators will help to efficiently explore and exploit the neighborhoods of the incumbent solution such that different solution structures can be investigated in the search iterations.

In summary, given $x_{ij}^{v}(S)$, $p_{ij}^{vw}(S)$, $\beta_{ij}^{v}(S)$, and $\lambda_{ij}^{v}(S)$ that denote the values of the corresponding variables in the incumbent solution S, the partial-MILP method is used to find a new neighbor solution S' as follows:

- **Step 1**: Select a subset $\mathbf{\Omega}$ of route and platoon variables, i.e., x_{ij}^{v}, p_{ij}^{vw}, β_{ij}^{v}, and λ_{ij}^{v}, by any neighbourhood search operator introduced above during each iteration;
- **Step 2**: Fix $x_{ij}^{v} \leftarrow x_{ij}^{v}(S)$, $p_{ij}^{vw} \leftarrow p_{ij}^{vw}(S)$, $\beta_{ij}^{v} \leftarrow \beta_{ij}^{v}(S)$, $\lambda_{ij}^{v} \leftarrow \lambda_{ij}^{v}(S)$ for all edge (i, j) and trucks v, w;
- **Step 3**: Unfix x_{ij}^{v}, p_{ij}^{vw}, β_{ij}^{v}, and λ_{ij}^{v} in set $\mathbf{\Omega}$;
- **Step 4**: Invoke the MIP solver to optimize the resultant MILP model and return a new solution S'.

The partial-MILP approach will be employed in a framework of iterated neighborhood search (INS) to be introduced in the following subsection. The performance of the five operators will be quantitatively analyzed and compared through the numerical experiments in Section 5.

4.2. Iterated neighborhood search

Starting from an initial solution, the INS will iteratively search for better solutions in the neighborhood identified by the aforementioned search operators in turn. Only one search operator will be used in each search iteration, and if the new solution found by the partial-MILP method is better than the incumbent solution, it will become a new incumbent solution for the next search iteration. A search operator will be used consecutively in many iterations until the partial-MILP method fails to find a better solution in the neighborhood defined by the operator, and in this case, the next search operator will be used. The iterative search will be terminated when no further improvement can be made to the incumbent solution after the pre-specified maximum number of iterations or maximum time for the whole search process. The incumbent solution will be the best solution found for the TRP problem.

The P-MILP-INS is outlined in Algorithm 1. As shown in the pseudocode, the algorithm begins with an initialization process to find a feasible incumbent solution S_0 by solving the model [TRP] without an objective function using a MIP solver. Meanwhile, the number of consecutive iterations that do not generate a better solution, denoted by B, is initialized to be 0. We will start from the first search operator by setting the operator index O to be 1. The number of times that the operator O has been used and the number of times that improvements have been made on the incumbent solution by operator O, represented by $U(O)$ and $I(O)$, respectively, are initialized to be 0 for each $O \in \{1,2,3,4,5\}$. Then, a loop is launched to implement the INS in Lines 2-24. In the INS loop, the partial-MILP method will be used to find a new neighbor solution following the step-by-step procedure in Subsection 4.1. Specifically, one of the five operators will be employed first to select node(s) or truck(s) and generate the corresponding set of unfixed variables in $\mathbf{\Omega}$ (see Lines 3-13). The route and platoon variables will then be fixed to be the values of the incumbent solution S (see Line 14). Finally, the variables in set $\mathbf{\Omega}$ will be unfixed, and the MIP solver will be invoked to solve the resultant MILP model and generate a new solution S'. If the new solution is better than the incumbent one, it will be accepted as the new incumbent solution, and the non-improvement counter B will be reset to 0 and the number of times that improvements have been made on the incumbent solution by the concerned operator O, i.e., $I(O)$, will be increased by one (see Line 18); otherwise, the search will move to the next operator, i.e., $O \leftarrow (O \bmod 5)+1$, and the non-improvement counter B is increased by one (see Line 19). The loop will stop if no further improvement can be made to the incumbent solution after $B_{\max}$ continuous attempts or the elapsed CPU time is larger than the maximum time limit $T_{\max}$ (see Lines 21-23). Finally, the incumbent solution will be the output of the algorithm as the best solution found. Note that in the INS loop, Lines 3-13 act as the 'shaking phase', and Line 16 serves as the local search using the MIP solver.

Algorithm 1. Pseudocode of the proposed P-MILP-INS

1 Initialization: Find S_0 by the MIP solver; $S \leftarrow S_0$; $B \leftarrow 0$; $U(O) \leftarrow 0$, $I(O) \leftarrow 0$, $\forall O \in \{1,2,3,4,5\}$; $O \leftarrow 1$.

2 Loop begins: repeat the following steps until the stopping condition is satisfied.

3 $\mathbf{\Omega} \leftarrow \varnothing$;

4 If $O = 1$, then

5   apply OP-1 to generate $\mathbf{\Omega}$; $U(O) \leftarrow U(O)+1$;

6 Else if $O = 2$, then

7   apply OP-2 to generate $\mathbf{\Omega}$; $U(O) \leftarrow U(O)+1$;

8 Else if $O = 3$, then

9   apply OP-3 to generate $\mathbf{\Omega}$; $U(O) \leftarrow U(O)+1$;

10 Else if $O = 4$, then

```
        apply OP-4 to generate Ω; U(O) ← U(O)+1;
    Else apply OP-5 to generate Ω; U(O) ← U(O)+1;
    EndIf
    Fix the variables based on S: x_ij^v ← x_ij^v(S), p_ij^vw ← p_ij^vw(S), β_ij^v ← β_ij^v(S),
        λ_ij^v ← λ_ij^v(S), ∀(i, j) ∈ E, v, w ∈ V;
    Unfix the variables x_ij^v, p_ij^vw, β_ij^v, and λ_ij^v in set Ω;
    Invoke the MIP solver to find a new neighbour solution S';
    If S' improves upon S, then
        S ← S'; B ← 0; I(O) ← I(O)+1;
    Else O ← (O mod 5)+1; B ← B+1;
    EndIf
    If B > B_max or the elapsed CPU time exceeds T_max, then
        Break: jump out of the loop and stop;
    EndIf
Loop end
Return the incumbent solution S.
```

5. Model extension

The model presented in Section 3 can effectively differentiate the fuel reduction rates of the truck traveling alone and that as the leader and follower of a platoon. However, the trucks in the following positions are assumed to experience the same fuel reduction rate and thereby the variation of the fuel reduction rates of the following trucks at different positions are not considered in the proposed model [TRP]. In fact, field tests have shown that the platoon followers also receive different aerodynamic benefits depending on their positions in the platoon (Lee et al., 2021; Michaelian and Browand, 2000). For example, the tail vehicle saved fuel by 7% while the interior vehicles traveling between the lead vehicle and the tail vehicle can save fuel by 10% thanks to the aerodynamic improvement from both the vehicles in front and behind the vehicle (Michaelian and Browand, 2000). Therefore, this subsection will present a more general model on top of model [TRP] that additionally considers different fuel-saving benefits for the interior truck(s) and tail truck within a platoon. As such, in addition to the variables and parameters introduced previously, we need define another type of platoon variables, i.e., the binary decision variables α_{ij}^{v} , $\forall (i,j) \in \mathbf{E}, v \in \mathbf{V}$, indicating whether truck v

is at the last position of a platoon when traversing edge (i,j). This variable is used to differentiate the interior truck traveling in the middle of a platoon and the tail truck of a platoon. Similar to Eqs. (6) and (13), we can readily obtain the following relationship between the route variables x_{ij}^{v} and the tail truck variables α_{ij}^{v} to restrict that a truck cannot be the tail truck of a platoon on an edge that is not traversed by that truck at all:

$$\alpha_{ij}^{v} \le x_{ij}^{v}, \quad \forall (i,j) \in \mathbf{E}, v \in \mathbf{V} \tag{31}$$

We then proceed to establish the relationship between p_{ij}^{vw} and α_{ij}^{v}. Since the value of α_{ij}^{v} is also jointly determined by A_{ij}^{v} and B_{ij}^{v}, we have the following information of α_{ij}^{v} :

$$\alpha_{ij}^{v} = \begin{cases} 0, & \text{if } A_{ij}^{v} = 0, B_{ij}^{v} \ge 1 \\ 0, & \text{if } A_{ij}^{v} \ge 1, B_{ij}^{v} \ge 1 \\ 1, & \text{if } A_{ij}^{v} \ge 1, B_{ij}^{v} = 0 \\ 0, & \text{if } A_{ij}^{v} = 0, B_{ij}^{v} = 0 \end{cases}, \quad \forall (i,j) \in \mathbf{E}, v \in \mathbf{V} \tag{32}$$

By consolidating the conditions in Eq. (32), we can find that α_{ij}^{v} would be 0 if either $B_{ij}^{v} \ge 1$ or $A_{ij}^{v} = 0$. Similar to the process for determining λ_{ij}^{v} in Subsection 2.3, we shall have the following constraints to equivalently express all the relationships in Eq. (32):

$$\alpha_{ij}^{v} \le A_{ij}^{v}, \quad \forall (i,j) \in \mathbf{E}, v \in \mathbf{V} \tag{33}$$

$$\alpha_{ij}^{v} \le 1 - \frac{B_{ij}^{v}}{M_3}, \quad \forall (i,j) \in \mathbf{E}, v \in \mathbf{V} \tag{34}$$

$$\alpha_{ij}^{v} \ge \frac{A_{ij}^{v}}{M_3} - B_{ij}^{v}, \quad \forall (i,j) \in \mathbf{E}, v \in \mathbf{V} \tag{35}$$

where Eq. (33) enforces α_{ij}^{v} to be 0 when $A_{ij}^{v} = 0$, Eq. (34) restricts α_{ij}^{v} to be 0 when $B_{ij}^{v} \ge 1$, and Eq. (35) forces λ_{ij}^{v} to be 1 when $A_{ij}^{v} \ge 1$ and $B_{ij}^{v} = 0$. In addition, it is straightforward to have the following constraint to establish the relationship between β_{ij}^{v} and α_{ij}^{v}:

$$\alpha_{ij}^{v} \le \beta_{ij}^{v}, \quad \forall (i,j) \in \mathbf{E}, v \in \mathbf{V} \tag{36}$$

which indicates that a truck cannot be the tail truck of a platoon over edge (i,j) if it is not even a following truck in the platoon over that edge. Kindly note that a following truck of a platoon can either be the tail truck traveling at the last position of this platoon or an interior truck traveling between the lead and the tail truck of the platoon. Therefore, if ($\beta_{ij}^{v} - \alpha_{ij}^{v}$) equals 1, it means that truck v is an interior truck of a platoon when traversing edge (i, j).

In summary, the extended model considering different fuel reduction rates of the following trucks at different positions is formulated as follows:

[TRP-E]

$$\min_{\mathbf{x},\mathbf{p},\boldsymbol{\alpha},\boldsymbol{\beta},\boldsymbol{\lambda},\mathbf{t},\mathbf{u}} \sum_{v \in \mathbf{V}} \sum_{(i,j) \in \mathbf{E}} c_{ij} \left[x_{ij}^{v} - \eta_{l} \lambda_{ij}^{v} - \eta_{f_i} \alpha_{ij}^{v} - \eta_{f_e} (\beta_{ij}^{v} - \alpha_{ij}^{v}) \right] \tag{37}$$

subject to Eqs. (1)-(7), (9)-(14), (16), (18)-(20), (22)-(29), (31), (33)-(36), and

$$\alpha_{ij}^{v} \in \{0,1\}, \quad \forall (i,j) \in \mathbf{E}, v \in \mathbf{V} \tag{38}$$

where η_{f_i} and η_{f_e} denote the fuel reduction rate for the interior truck and the tail truck of a platoon, respectively. The objective function in Eq. (37) is the total incurred fuel cost with additional consideration of different fuel-saving rates of the interior truck and tail truck of a platoon. Constraints (1)-(7), (9)-(14), (16), (18)-(20), (22)-(27) and (29) have been elaborated in Subsection 3, while Constraints (31) and (33)-(36) have been elaborated above in this subsection. Constraint (38) define the domain of the binary decision variables.

We can find that the incorporation of different fuel reduction rates of the following vehicles at different positions in a platoon does not affect the model property and thus the proposed P-MILP-INS algorithm is still applicable except that we now have four types of platoon variables.

6. Numerical experiments

This section presents the results of a series of computational experiments on randomly generated instances. First, we will introduce the test instances used for our tests. We will then evaluate the performance of the proposed model and the P-MILP-INS algorithm. Finally, sensitivity analysis is conducted to explore the impacts of the fuel reduction of the leading vehicle of the platoon, drivers' mandatory breaks, and the width of the service time window on the system performance. The algorithm is coded in AMPL calling IBM ILOG CPLEX 12.9 on a personal computer with Intel (R) Core (TM) i7 3.4GHz CPU with 16 GB RAM.

6.1. Test instances

A total of 6 bidirected highway networks with different combinations of the node number and the topology complexities measured by the ratio of edge number to node number, i.e., $|\mathbf{N}| \in \{10, 30, 50\}$ and $|\mathbf{E}|/|\mathbf{N}| \in \{2.5, 5.0\}$, are randomly generated. The travel time on edge (i, j), i.e., w_{ij}, measured by minute, is randomly chosen as an integer from the set {5, 6, 7, …, 30}. Figure 2 illustrates some examples of randomly generated networks with different node numbers and topology complexities. As for the truck fleet, for simplicity, each truck is assumed to have only one intermediate relay node denoted by i_v. The origin, destination, and relay node of each truck are randomly generated from the node set of the networks. Besides, the required relay time for each truck at the designated relay node, i.e., e^v, is an integer randomly drawn from the set {1, 2, …, 10}. The earliest departure time for each truck, i.e., σ_v, is uniformly drawn from the set {0, 1, 2, …, 30}, while the corresponding latest arrival time is set to be

$$\tau_v = \sigma_v + (1+\varphi)(\chi_{o_v i_v} + \chi_{i_v d_v} + e^v), \quad \forall v \in \mathbf{V} \tag{39}$$

where $(\chi_{o_v i_v} + \chi_{i_v d_v} + e^v)$ is the shortest travel time from the origin to the destination of truck v considering the relay requirement and φ is a parameter to control the width of the service time window. Unless stated otherwise, φ is set to be 0.5. The mandatory break time for each truck driver T_v is set to a percentage of the shortest travel time as follows:

$$T_v = \varsigma(\chi_{o_v i_v} + \chi_{i_v d_v} + e^v), \quad \forall v \in \mathbf{V} \tag{40}$$

where the percentage ς is set to be 20%. The fuel cost of a travel-alone truck on each edge is set to be the same as the travel time on that edge. The fuel reduction rates of the leading and following trucks in a platoon, i.e., η_l and η_f, are assumed to be 8% and 16%, respectively (Davila et al., 2013). The threshold for platoon size on all edges is set to be 6. Regarding the algorithm-related parameters, we set $W_1 = 5$ and $W_2 = 5$ based on our preliminary experiments. The stopping criteria of the P-MILP-INS algorithm are set to be $T_{\max} = 2$ hr and $B_{\max} = 10$.

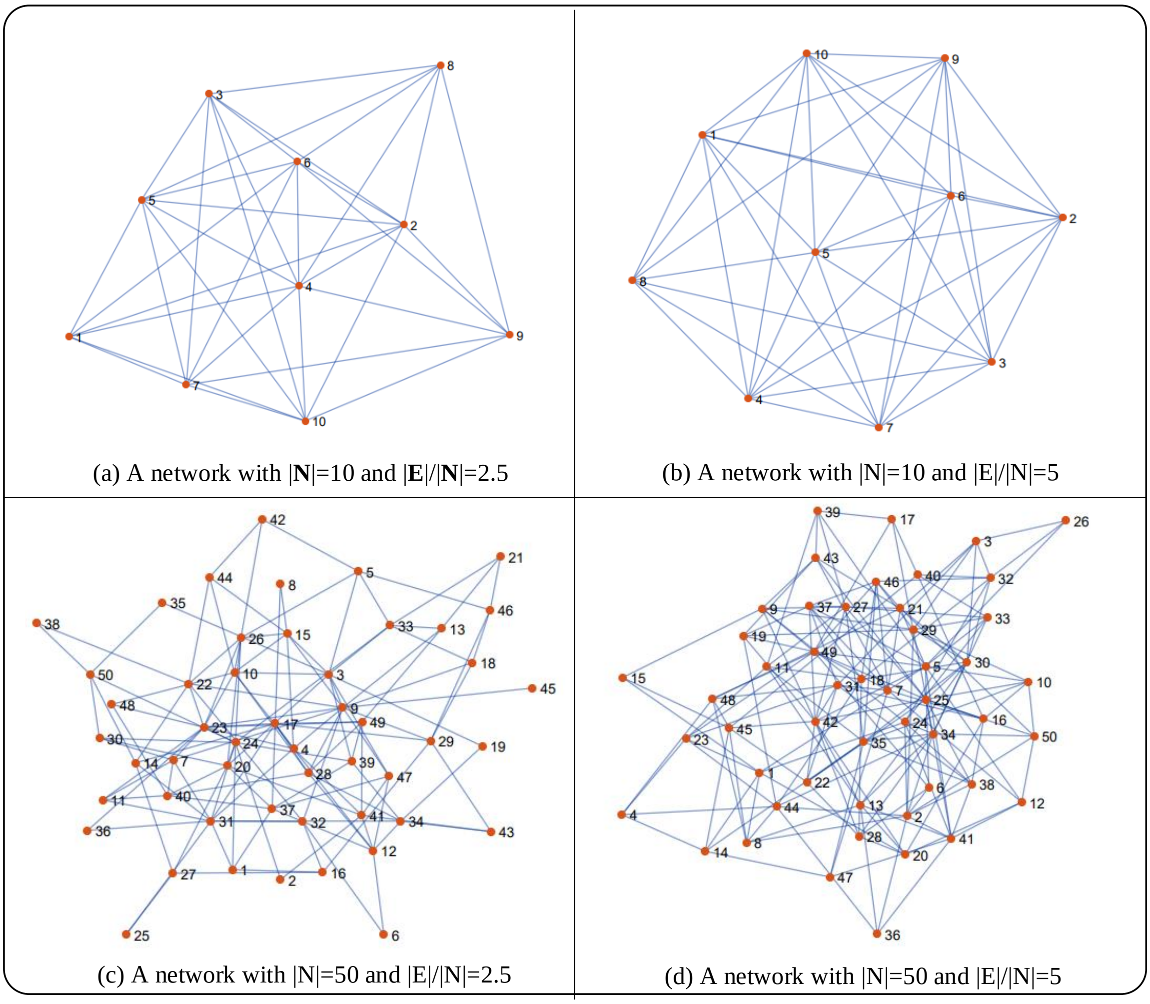

(a) A network with |**N**|=10 and |**E**|/|**N**|=2.5

(b) A network with |N|=10 and |E|/|N|=5

(c) A network with |N|=50 and |E|/|N|=2.5

(d) A network with |N|=50 and |E|/|N|=5

Figure 2. Examples of randomly generated highway networks

6.2. Algorithm performance

Comparison of P-MILP-INS and CPLEX

To evaluate the performance of the proposed solution method, we will compare the results of the proposed P-MILP-INS algorithm with those obtained by solving the [TRP] model directly using CPLEX. Other than the network node number and the topology complexity, the fleet size is expected to largely influence the model size and, accordingly, the computational efficiency of the solution method. Therefore, we consider 5 fleet scenarios with different numbers of trucks, i.e., $|\mathbf{V}| \in \{10, 20, 30, 40, 50\}$ in each of the aforementioned 6 networks. Given the highway network topology and the truck fleet size, 5 instances with the above randomly generated parameters will be created. As such, a total of 150 instances will be used to assess the model and solution method. A limit of 2 hr is imposed for solving each of these instances in CPLEX. In other words, for a specific instance, CPLEX will stop if either an optimal solution has been obtained within 2 hr or the elapsed time exceeds 2 hr.

Table 1 shows the results of the proposed P-MILP-INS algorithm and CPLEX under various fleet sizes in networks with different node numbers and topology complexities. For both methods, we report the best objective function values obtained within the time limit (Obj) and the CPU times used to obtain the solutions (CPU Time). We will also report the number of instances solved to optimality by CPLEX (#Solved). It shows that the proposed P-MILP-INS algorithm can find the solutions for all the instances within 0.5 hr on average. On the contrary, CPLEX fails to identify even a feasible solution for most instances within 2 hr, and it only manages to solve the smallest instances with no more than 10 trucks in networks with 10 nodes. In addition, for these small instances that are solved to optimality by CPLEX, the proposed P-MILP-INS algorithm obtains the same optimal solutions with much less time than CPLEX, e.g., 17s v.s. 2,853s for instances with $|\mathbf{V}|=10$, $|\mathbf{N}|=10$, and $|\mathbf{E}|/|\mathbf{N}|=2.5$. The findings show the computational challenge of the proposed TRP problem when solved directly by CPLEX and the efficacy of the proposed algorithm to address the underlying problem in terms of solution quality and computational efficiency. Moreover, if we dig deeper, we will see that the computation times of both the proposed algorithm and CPLEX seem more sensitive to the fleet size and the network node number than to the topology complexity. For example, for instances with $|\mathbf{V}|=40$ and $|\mathbf{E}|/|\mathbf{N}|=2.5$, the CPU time of the P-MILP-INS algorithm has increased more than 2 times from 1,865s to 4,988s when the network node number changes from 30 to 50, whereas the average CPU time only increases slightly from 1,688 to 1,782 when

Table 1. Comparison of the proposed P-MILP-INS algorithm and CPLEX

$\|\mathbf{V}\|$	$\|\mathbf{N}\|$	$\|\mathbf{E}\|/\|\mathbf{N}\|=2.5$					$\|\mathbf{E}\|/\|\mathbf{N}\|=5$				
		P-MILP-INS		CPLEX			P-MILP-INS		CPLEX		
		Obj	CPU Time (s)	Obj	CPU Time (s)	#Solved	Obj	CPU Time (s)	Obj	CPU Time (s)	#Solved
10	10	576	17	576	2,853	5	592	17	592	3,219	5
	30	1,037	68	-	7,200	0	1,066	80	-	7,200	0
	50	1,782	362	-	7,200	0	1,689	394	-	7,200	0
20	10	1,351	51	-	7,200	0	1,421	67	-	7,200	0
	30	1,534	584	-	7,200	0	1,474	726	-	7,200	0
	50	2,773	1,129	-	7,200	0	2,852	930	-	7,200	0
30	10	2,393	209	-	7,200	0	2,593	196	-	7,200	0
	30	2,782	1,175	-	7,200	0	2,888	1,191	-	7,200	0
	50	3,237	2,782	-	7,200	0	3,341	2,922	-	7,200	0
40	10	3,292	301	-	7,200	0	3,632	312	-	7,200	0
	30	3,627	1,865	-	7,200	0	3,564	1,963	-	7,200	0
	50	3,857	4,988	-	7,200	0	4,004	5,640	-	7,200	0
50	10	4,861	1,735	-	7,200	0	4,994	1,583	-	7,200	0
	30	5,141	3,075	-	7,200	0	4,990	3,582	-	7,200	0
	50	5,210	6,976	-	7,200	0	5,516	7,134	-	7,200	0
Average		-	1,688	-	-	-	-	1,782	-	-	-

the topology complexity grows from 2.5 to 5. Similar examples can be found for the fleet size as well. To further examine the impacts of the two most influential factors on the computational efficiency of the proposed algorithm, we visualize the variations of the average CPU times of the P-MILP-INS algorithm with respect to the fleet size and the network node number in Figure 3 (a) and (b), respectively. It shows that the CPU time increases in a 'semi-exponential' way lying in between the linear and exponential trends. This is within our expectation: since the proposed algorithm integrates the partial-MILP method and INS, it inherits the characteristics of formulation-based heuristics (good solution quality but with exponentially growing computation time) and metaheuristics (with linearly increasing time). The proposed algorithm lays an ideal framework to strike a good balance between solution quality and computational efficiency by constructing a set of unfixed variables of reasonable size in real-world applications.

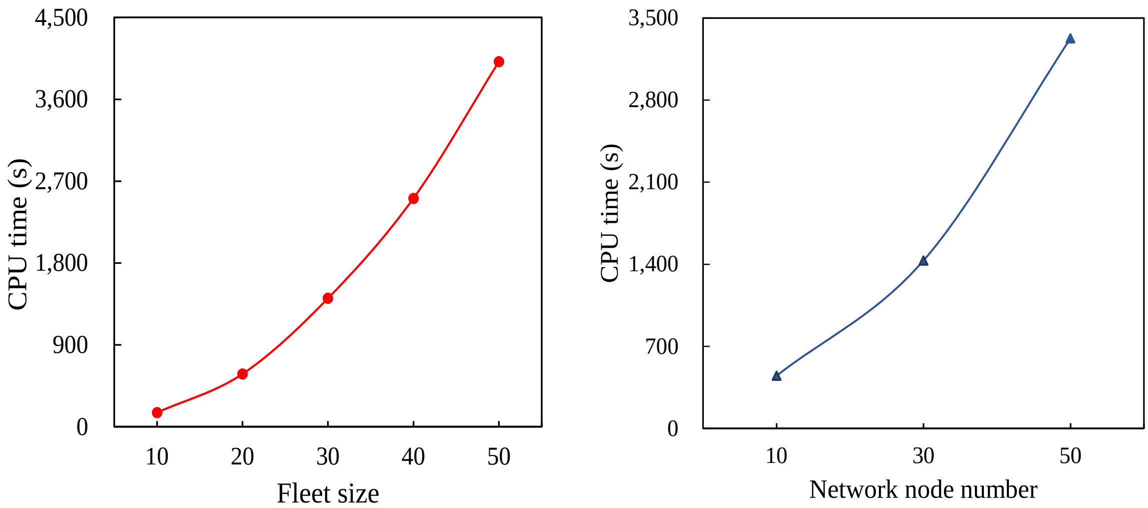

(a) Variations of the average CPU times with the increase of the fleet size

(b) Variations of the average CPU times with the increase of the network node number

Figure 3. Variations of the average CPU times of the P-MILP-INS algorithm with the increase of the fleet size and network node number

Comparison of neighborhood search operators

We further evaluate the performances of the five tailor-made neighborhood search operators used in the P-MILP-INS algorithm for solving the TRP problem. The effectiveness of each operator is measured by the average improvement ratio (AIR) $I(O)/U(O)$, i.e., the ratio of the number of times that the operator improves the incumbent solution to the number of times that the operator has been used, for each group of instances with the same fleet size, network node number, and topology complexity. The results are tabulated in Table 2. Overall, it shows that all the five tailor-made neighborhood search operators have significant effects on improving the incumbent solution in the course of the P-MILP-INS algorithm, with the average AIRs being at or above 0.13. It is also interesting to find that the OP-5 has the best performance among all the operators in terms of the average AIR, followed by the OP-4, OP-3, OP-2, and OP-1 in sequence. On the one hand, the results suggest that the truck-based operators are more effective than the node-based ones in identifying better neighborhood solutions. This could be attributed to the greater spatial synergies among the unfixed variables for a truck. On the other hand, it can be seen that for both the node-based and truck-based operators, the operators considering the nearest nodes/trucks show better performances. As expected, compared with random node selection in OP-1, the selection of node clusters in OP-2 is more likely to find promising routing and platooning plans. For the truck-based operators, both the increased number of unfixed variables and the consideration of spatiotemporal closeness contribute to the improved performance of OP-5 over OP-4, followed by OP-3.

Based on the above findings, we proceed to analyze the impacts of fleet size, network node number, and topology complexity on the performance of the five operators. Specifically, for the topology complexity, it is notable to see that the increased topology complexity does not necessarily lead to a decreased AIR. Take OP-4 in instances with $|\mathbf{V}|=10$ and $|\mathbf{N}|=50$ for example, the AIR increases from 0.20 to 0.32 when the topology complexity grows from 2.5 to 5. We further conduct the paired t-test to statistically examine if the AIRs for instances with $|\mathbf{E}|/|\mathbf{N}|=2.5$ and $|\mathbf{E}|/|\mathbf{N}|=5$ are significantly different from each other. The p-value is 0.80, larger than the standard significance level of 0.05, so the results do not support the hypothesis that the performances are different in networks with distinct complexities. As for the other two factors, we show the variations of the average AIR with the increase of fleet size and network node number in Figure 4 (a) and (b), respectively. According to Figure 4 (a), the performances of the node-based operators are negatively affected by the fleet size, while the truck-based operators, in general terms, show improved performance for a larger fleet. Notably, the average AIR of OP-1 has reduced to be less than 10% in instances with 50 trucks. Nevertheless, it has increased to 40% for OP-5, demonstrating the increasingly competitive advantages of the truck-based operators, especially OP-5, over the node-based ones in large-fleet problems that are computationally intensive. When it comes to the network size, similar findings can be observed in Figure 4 (b), in which the node-based and truck-based operators show the downward and upward trend performances, respectively, with the increase of network node number. Compared to the fleet size, the performances of these operators are less sensitive to the changes of network node number as the variations of AIR are smaller in magnitude.

Table 2. Comparison of the neighborhood search operators

Instance			Average improvement ratio				
$\|\mathbf{V}\|$	$\|\mathbf{N}\|$	$\|\mathbf{E}\|/\|\mathbf{N}\|$	OP-1	OP-2	OP-3	OP-4	OP-5
10	10	2.5	0.22	0.21	0.21	0.24	0.24
		5	0.21	0.20	0.25	0.23	0.23
	30	2.5	0.20	0.17	0.23	0.21	0.24
		5	0.17	0.17	0.22	0.22	0.31
	50	2.5	0.14	0.16	0.21	0.20	0.27
		5	0.13	0.22	0.23	0.32	0.36
20	10	2.5	0.12	0.22	0.24	0.28	0.28
		5	0.20	0.19	0.22	0.31	0.27
	30	2.5	0.18	0.16	0.22	0.36	0.34
		5	0.15	0.16	0.28	0.31	0.36
	50	2.5	0.15	0.17	0.29	0.34	0.37
		5	0.14	0.13	0.28	0.36	0.40
30	10	2.5	0.12	0.18	0.27	0.34	0.31
		5	0.19	0.18	0.26	0.30	0.30
	30	2.5	0.13	0.17	0.27	0.29	0.30
		5	0.13	0.16	0.23	0.32	0.29
	50	2.5	0.12	0.18	0.27	0.30	0.35
		5	0.09	0.16	0.30	0.35	0.35
40	10	2.5	0.14	0.19	0.27	0.29	0.34
		5	0.13	0.10	0.31	0.29	0.43
	30	2.5	0.11	0.16	0.26	0.30	0.31
		5	0.10	0.16	0.30	0.28	0.35
	50	2.5	0.08	0.13	0.29	0.35	0.42
		5	0.08	0.16	0.29	0.37	0.39
50	10	2.5	0.11	0.13	0.35	0.39	0.34
		5	0.07	0.12	0.29	0.31	0.40
	30	2.5	0.10	0.11	0.33	0.32	0.41
		5	0.11	0.10	0.30	0.34	0.39
	50	2.5	0.04	0.08	0.31	0.38	0.43
		5	0.04	0.09	0.29	0.39	0.42
Average			0.13	0.16	0.27	0.31	0.34

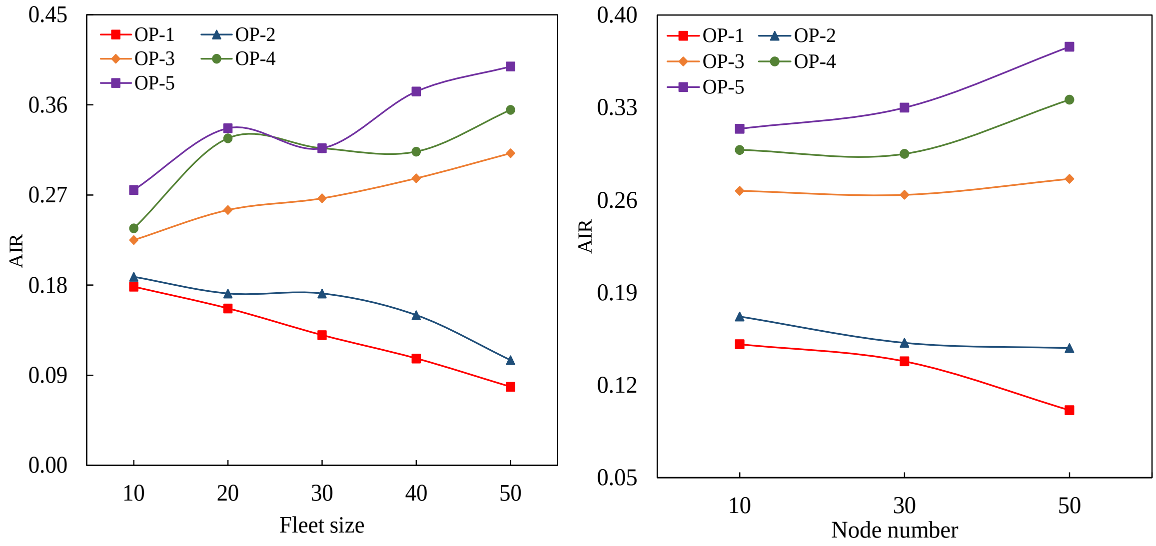

(a) Variations of AIR with the increase of the fleet size (b) Variations of AIR with the increase of node number

Figure 4. Variations of AIR with the increase of the fleet size and network node number

6.3. Results comparison to the extended model

To explore the impact of considering different fuel-saving effects for the interior truck and the tail truck of a platoon on the system performance in terms of the total fuel cost (FC), the travel time (TT), the platooning time (PT), as well as the platoon length (PL), we compare the solutions to the original model [TRP] with those of the extended model [TRP-E] in three groups of instances with $\eta_l = 8\%$, $\eta_{f_i} = 16\%$, and $\eta_{f_e} = 12\%$. The results are summarized in Table 3. It shows that the total fuel cost considering the reduced fuel saving of the tail truck of a platoon will increase; nevertheless, the influence is not significant in small and middle instances since the indicator values under the two models does not differ too much. For example, the difference of the total fuel cost in the instances with $|\mathbf{V}|=10$, $|\mathbf{N}|=10$ is only $23. Moreover, we find that the consideration of different fuel reduction rates for the interior trucks and the tail truck may also affect the routing and platooning plans, especially in large instances. More specifically, comparatively speaking, the consideration of lower fuel reduction rate of the tail truck may discourage platoon formation, which can be reflected by the decrease of the platooning time and the increase of the total fuel cost in instances with $|\mathbf{V}|=50$, $|\mathbf{N}|=50$. This may be attributed to the fact that some platooning plans under the model [TRP] may not be cost effective for the model [TRP-E]. In addition, we also find that the comparatively lower fuel reduction rate of the tail truck may foster the formation of longer platoons since a larger average platoon length has been obtained under the model [TRP-E]. This can be explained by the fact that more small platoons mean more tail trucks and thus less fuel savings.

Table 3. Comparison of the original model [TRP] with the extended model [TRP-E]

$\|\mathbf{V}\|$	$\|\mathbf{N}\|$	TRP				TRP-E			
		FC ($)	TT (min)	PT (min)	PL	FC ($)	TT (min)	PT (min)	PL
10	10	592	74.24	48.56	2.50	615	74.24	48.56	2.50
30	30	2,452	89.44	65.69	2.83	2,557	90.32	64.89	2.85
50	50	5,516	114.93	88.64	3.52	5,846	116.49	87.64	3.66

6.4. Sensitivity analysis

In this subsection, we will explore the impacts of the drivers' mandatory breaks, the fuel reduction rate of the leading truck of a platoon, and the width of service time window on the system performance in terms of the cost, i.e., the total fuel cost (FC) and various time-related indicators, including the travel time (TT), the platooning time (PT), the travel-alone time (AT), the dwell time (DT), the leading time (LT), the following time (FT) of trucks, as well as the break time (BT) of drivers. For the time-related parameters, we report both the mean time averaged over each truck/driver and the time variance (for the leading time, the following time, and the break time only) that measures the spread between times of all the trucks/drivers. The sensitivity analysis is carried out in the instances with $|\mathbf{V}|=30, |\mathbf{N}|=30$, and $|\mathbf{E}|/|\mathbf{N}|=5$.

Impact of drivers' mandatory breaks

To investigate the impact of drivers' mandatory breaks on the system performance, we will compare the values of the total fuel cost and time-related indicators under different mandatory break times in Eq. (40), i.e., $\varsigma \in \{0, 10\%, 20\%, 30\%\}$, in the aforementioned instances. The results are summarized in Table 4. It shows the negative impact of the break time requirement on the total fuel cost. This can be explained by the additional restriction imposed by Eq. (10), making some cost-effective routing and platooning plans unfeasible in break times. This is consistent with our expectation and the findings in previous studies that the consideration of drivers' breaks will deteriorate the fuel-saving benefit of platooning. Fortunately, we can find that the total fuel cost under $\varsigma = 10\%$ remains almost the same as that when there is no break time requirement. This means that the influence is not significant when the break time requirement is not stringent. Even if we have $\varsigma = 30\%$, i.e., taking an 18-min break for every 1 hr's driving, the total fuel cost reduces 1.25% only. In fact, the allowance of rest in the trucks' following times and relays has eased the restriction of the break time requirement. As for the time-related indicators, we find different travel times and platooning times, indicating that the routing and platooning plan should be adjusted to accommodate the break time requirement. These indicators appear insensitive to the break time restrictions with small values of ς unless it has reached 20% or above, in which case the trucks have more time to travel alone instead of in the form of a platoon.

Table 4. Effect of drivers' mandatory breaks on the system performance

ς	Cost ($)	Mean time (min)							Time variance (min^2)		
	FC	TT	PT	AT	DT	LT	FT	BT	LT	FT	BT
0	2,442	88.88	69.42	19.46	22.90	24.87	44.55	67.45	24.53	39.14	215.42
10%	2,443	89.22	69.96	19.26	23.49	23.66	46.30	69.79	23.54	32.50	211.45
20%	2,452	89.44	65.69	23.75	27.56	22.91	42.78	70.34	24.82	29.13	188.09
30%	2,473	90.47	64.94	25.53	31.78	24.23	40.71	72.49	24.53	28.81	108.63

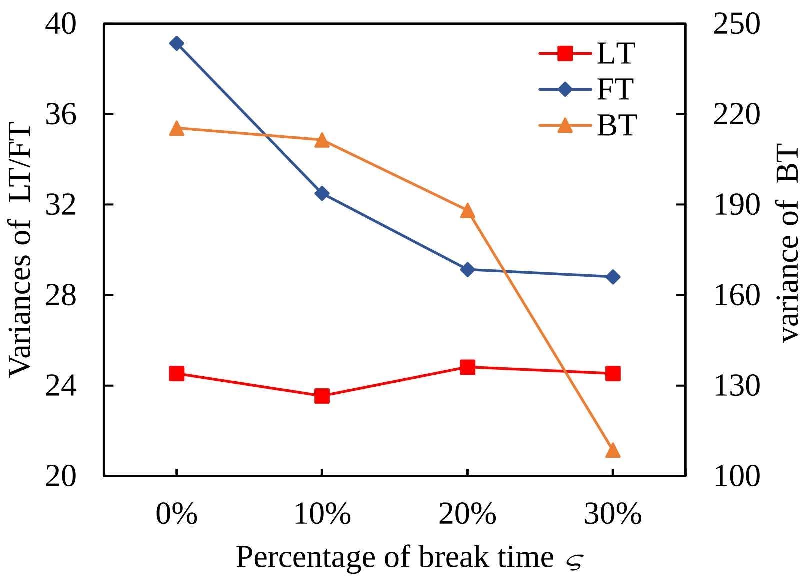

Figure 5. Variations of the variances of the leading, following, and break times under different break time requirements

Although both the following time and dwell time can be used as the break times, the high requirement for break times stimulates the increase of the dwell time only. The platooning time, more exactly, the following time, however, reduces with the increasing requirement for drivers' breaks. This is somehow out of our expectations. Probably to comply with the break time requirement, some trucks have to switch to other routes with fewer platooning opportunities; and the increment of dwell time has nothing to do with the platooning formation and is for the purpose of rest only. Regarding the variances, Figure 5 shows that both the variances of the following time and break time have decreased with the increasing level of the break time requirement. A notable observation is that the variance of break time has been reduced by half under instances with $\varsigma = 30\%$. It is encouraging to find that the high requirement for drivers' breaks helps to achieve fair distributions of break times at no significant cost.

Impact of fuel reduction rate of the leading truck

For the fuel reduction rate of the leading truck, we will examine the solutions to the TRP problem under different fuel reduction rates of the leading truck $\eta_l \in \{0, 0.04, 0.08, 0.12\}$. The results are tabulated in Table 5. It shows that the total fuel cost will decline steadily with the increase of the fuel reduction rate of the leading truck. Notably, by factoring in the fuel reduction of the leader at the rate $\eta_l = 0.12$, the total fuel cost can be reduced by nearly 5% (calculated by (2,513-2,393)/2,513). The additional fuel savings resulted from not only the direct fuel reduction of the leading trucks but also the more cost-effective routing and platooning plans obtained by incorporating this factor in the model building and algorithm design for the TRP problem. It can be seen in Table 5 that we actually obtain distinctive route and platoon plans associated with different travel and platooning times under different fuel reduction rates. Moreover, similar to drivers' mandatory breaks, the fuel reduction rates influence the time-related indicators somehow in a step-wise manner. It can be seen that the means of these indicators show no obvious variation with the increase of the fuel reduction rate until it reaches 12%. In this case, a visible increase in platooning time coupled with the reduction in travel-alone time and the great increment of dwell time can be observed. The findings suggest that the platooning plans will not differ too much unless the fuel reduction of the leading truck in the platoon becomes significant, and the high fuel savings of the leading trucks will render some unfavorable platooning opportunities viable with more waiting time at some nodes to form platoons.

Table 5. Effect of the fuel reduction rate of the leading truck on the system performance

η_l	Cost ($)	Mean time (min)							Time variance (min^2)		
	FC	TT	PT	AT	DT	LT	FT	BT	LT	FT	BT
0	2,513	90.20	69.57	20.64	28.05	22.38	47.18	75.23	29.49	43.95	246.34
4%	2,490	89.58	68.44	21.14	28.37	24.73	43.71	72.08	29.60	42.50	215.62
8%	2,452	89.44	69.06	20.38	25.56	25.91	43.15	68.70	24.82	29.13	188.09
12%	2,393	89.53	72.73	16.80	46.54	27.93	44.80	91.34	24.11	23.50	177.13

We further depict the changes of the variances of the leading, following, and break times against the fuel reduction rates in Figure 6. It shows that the variances of all the three time-related indicators decrease with the increase of the fuel reduction rate. This implies that more sensible routing and platooning plans with a fairer distribution of fuel-saving benefits and break times among the trucks and the drivers, respectively, can be obtained, if the fuel reduction rates of the leading trucks are large. Nevertheless, it is worthwhile to mention that there still exists a noteworthy unbalanced distribution of break times reflected by a much larger variance than those of the other two indicators. More thoughtful models aiming at a fair distribution of break times for the drivers can be developed in the future.

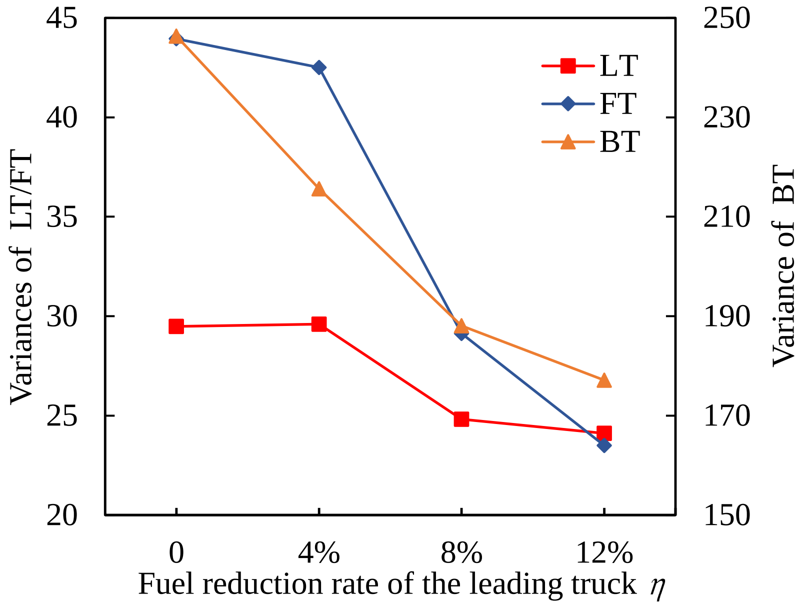

Figure 6. Variations of the variances of the leading, following, and break times under different fuel reduction rates of the leading truck

Impact of the width of the service time window

To explore how the width of the service time window affects the system performance, we will analyze the solutions for the TRP problem with different tightness of the time window by setting $\varphi \in \{0.5, 0.75, 1, 1.25\}$ in Eq. (39). The results are presented in Table 6. It is obvious to find that the total fuel cost constantly reduces with the increased width of the service time window. The result aligns with our expectation: if the deadline is not pressing, the trucks will have more freedom to choose longer (of course, it requires more time to reach the destinations) but more cost-saving routes with more platooning opportunities. This can be verified by the longer travel times and platooning times under large values of φ, e.g., 1 and 1.25, in Table 6. We also notice that the reduction of fuel cost is not uniform with respect to the change of width of the service time window. It shows relatively slow reduction rates under tight and slack time window constraints but a fast reduction rate under moderate time window constraints. A similar trend can be found in platooning time as these cost savings largely resulted from platooning. However, we caution that there should be a threshold beyond which further relaxation of time window constraints will not lead to cost savings. Among the other time-related indicators, the dwell time shows obvious increases under large service time windows because more waiting time is needed to coordinate trucks to form/join platoons, the number of which becomes larger than that in the cases with tight time window constraints. As a result, the break time of drivers increases accordingly. As for the variances, we can see from Figure 7 that the sharp increase of the variance of the break time almost doubles when φ increases from 0.5 to 1.25, while the variations for the leading and following time are marginal. The above findings imply that the relaxation of time window constraints could lead to more fuel savings and average more break time for drivers. However, these benefits do not come for free as it also results in a much more dispersed distribution of break time across drivers.

Table 6. Effect of the width of the service time window on the system performance

φ	Cost ($)	Mean time (min)							Time variance (min^2)		
	FC	TT	PT	AT	DT	LT	FT	BT	LT	FT	BT
0.5	2,452	89.44	69.06	20.38	25.56	23.91	45.15	70.70	24.82	29.13	188.09
0.75	2,439	90.66	70.60	20.06	29.57	24.20	46.40	75.97	24.60	34.72	230.84
1	2,397	91.89	75.68	16.21	33.13	26.58	49.09	82.22	24.75	34.54	274.75
1.25	2,383	93.48	76.99	16.49	38.52	27.87	49.11	87.63	24.50	32.19	360.27

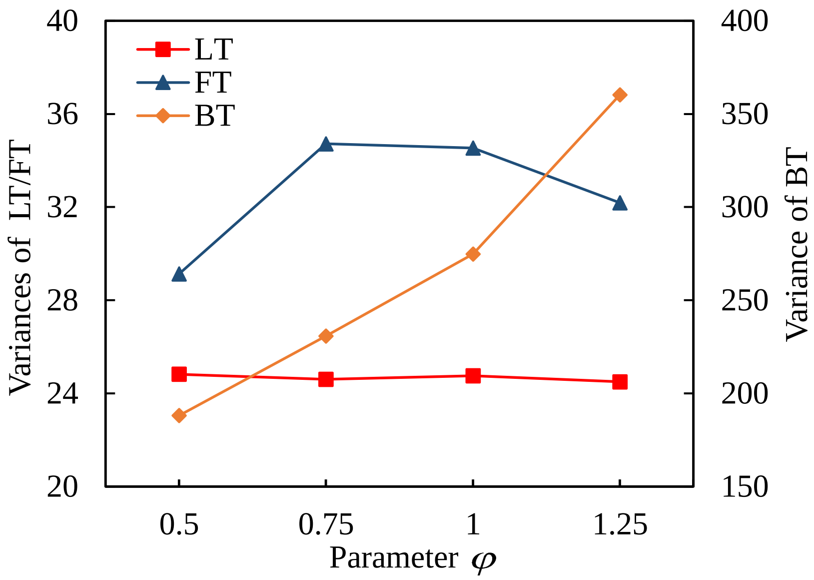

Figure 7. Variations of the variances of the leading, following, and break time under different widths of the service time windows

7. Conclusions

This study investigates the truck routing and platooning optimization problem considering the drivers' mandatory breaks, state-and-position-dependent fuel reduction rates, and trucks' designated relays for long-haul freight transportation. Drivers are required to take mandatory breaks, either by dwelling at road intersections or trailing behind some trucks in platoons, for safe driving over the long journeys. The fuel reduction rates of trucks are assumed to vary with their states and positions. Trucks should visit intermediate relay nodes to conduct necessary maintenance checks or delivery/pick-up tasks. To determine the optimal routing and platooning plan of the truck fleet that minimizes the total fuel cost over the entire trip, we formulated a novel MILP model that can effectively differentiate the travel-alone trucks from the leading trucks of platoons and incorporate the drivers' mandatory breaks and intermediate relay constraints. Due to the complicated structure of the proposed model, a customized partial-MILP method with iterated neighborhood search was proposed to obtain good-quality solutions to the underlying problem. Extensive numerical experiments were conducted to validate the efficacy of the proposed model and algorithm and to examine the impacts of several influential factors on the system performance.

Future research work can be undertaken in several aspects. First, the proposed solution method is not computationally efficient for large networks, which limits its applicability in real-world scenarios. Therefore, it is highly expected to develop more efficient solution methods that can produce good-quality solutions in much less time. Second, since trucks and drivers in different platoon positions benefit differently in terms of fuel savings and driving experience, more studies are necessary to address the benefit redistribution among platoon members and drivers to facilitate the formation of reliable and fair platoons. Last but not least, the mathematical model in this study can be extended by incorporating parameter uncertainty arising in real-time planning, such as traffic congestion and time-dependent travel times in the future.

Acknowledgements

The work described in this paper was supported by a grant from the Research Grants Council of the Hong Kong Special Administrative Region, China (Project No. PolyU 15221821) and a grant from the Research Committee of The Hong Kong Polytechnic University under project code ZVTK. The third author would like to thank the support from the National Science Foundation of the United States (CNS-1837245 and CMMI-1904575).

Appendix: Notations

Indices and sets:	
$\mathbf{G} = (\mathbf{N}, \mathbf{E})$	Graph with node set $\mathbf{N}$ and edge set $\mathbf{E}$
$\mathbf{N}$	Set of nodes
$\mathbf{E}$	Set of edges
$\mathbf{V}$	Set of trucks

$\mathbf{N}^v$ — Set of designated intermediate relay nodes of truck v

i, j — Indices for nodes

(i, j) — Index for edges

v, w — Indices for trucks

o_v — Index for origin node of truck $v \in \mathbf{V}$

d_v — Index for destination node of truck $v \in \mathbf{V}$

Known parameters:

σ_v — Earliest departure time for truck $v \in \mathbf{V}$

τ_v — Latest arrival time for truck $v \in \mathbf{V}$

w_{ij} — Time required to traverse edge (i, j)

e_i^v — Relay time at node $i \in \mathbf{N}^v$ for truck $v \in \mathbf{V}$

c_{ij} — Fuel cost of traversing edge (i, j)

T_v — The mandatory break time of the driver of truck $v \in \mathbf{V}$ during the entire journey

η_l — Fuel reduction rate of the leading truck in a platoon

η_f — Fuel reduction rate of the following trucks in a platoon

η_{f_i} — Fuel reduction rate for the interior truck of a platoon

η_{f_e} — Fuel reduction rate for the tail truck of a platoon

φ — Parameter to control the width of the service time window

ς — Parameter to adjust the mandatory break time for each driver

L_{ij} — Maximum platoon size on edge (i, j)

ζ_{vw} — Composite distance between truck $v \in \mathbf{V}$ and truck $w \in \mathbf{V}$

χ_{ij} — Shortest travel time from node $i \in \mathbf{N}$ to node $j \in \mathbf{N}$

Decision variables:

x_{ij}^v — Binary variable indicating whether truck $v \in \mathbf{V}$ will traverse edge (i, j)

p_{ij}^{vw} — Binary variable indicating whether truck $v \in \mathbf{V}$ will follow truck $w \in \mathbf{V}$ over edge (i, j)

α_{ij}^v — Binary variable indicating whether truck $v \in \mathbf{V}$ is at the last position of a platoon when traversing edge (i, j)

β_{ij}^v — Binary variable indicating whether truck $v \in \mathbf{V}$ is a following truck in a platoon over edge (i, j)

λ_{ij}^v — Binary variable indicating whether truck $v \in \mathbf{V}$ will lead a platoon over edge (i, j)

t_i^v — Time instant that truck $v \in \mathbf{V}$ starts traversing an edge from node $i \in \mathbf{N}$

u_i^v	Waiting time of truck $v \in \mathbf{V}$ at node $i \in \mathbf{N}$

References

Abdolmaleki, M., Shahabi, M., Yin, Y., Masoud, N., 2021. Itinerary planning for cooperative truck platooning. Transportation Research Part B: Methodological 153, 91-110.

Abdulahovic, A., Edlund, F., 2018. Designing a Back-Office System for Platooning.

ACEA, 2018. European automobile manufacturers' association. https://www.acea.auto/files/Platooning_roadmap.pdf

Bhoopalam, A.K., Agatz, N., Zuidwijk, R., 2018. Planning of truck platoons: A literature review and directions for future research. Transportation Research Part B: Methodological 107, 212-228.

Bhoopalam, A.K., Berg, R., Agatz, N., Chorus, C., 2021. The long road to automated trucking: Insights from driver focus groups. https://papers.ssrn.com/sol3/papers.cfm?abstract_id=3779469.

Bono, B., Tipping, A., Benigni, T., 2018. Industrial mobility: How autonomous vehicles can change manufacturing. https://www.pwc.com/us/en/industrial-products/publications/assets/pwc-industrial-mobility-and-manufacturing.pdf.

Boysen, N., Briskorn, D., Schwerdfeger, S., 2018. The identical-path truck platooning problem. Transportation Research Part B: Methodological 109, 26-39.

Davila, A., Aramburu, E., Freixas, A., 2013. Making the best out of aerodynamics: Platoons. SAE Technical Paper.

Fagnant, D.J., Kockelman, K., 2015. Preparing a nation for autonomous vehicles: opportunities, barriers and policy recommendations. Transportation Research Part A: Policy and Practice, 77, 167-181.

FMCSA (Federal Motor Carrier Safety Administration), 2011. Hours of service of drivers. https://www.fmcsa.dot.gov/regulations/rulemaking/2011-32696.

Gibraltarlaws, 2021. Regulation (EC) No 561/2006 of the European Parliament and of the Council. https://www.gibraltarlaws.gov.gi/legislations/regulation-ec-no-5612006-5513/version/01-01-2021.

Goel, A., Rousseau, L. M., 2012. Truck driver scheduling in Canada. Journal of Scheduling, 15(6): 783-799.

Goñi-Ros, B., Schakel, W.J., Papacharalampous, A.E., Wang, M., Knoop, V.L., Sakata, I., van Arem, B., Hoogendoorn, S.P., 2019. Using advanced adaptive cruise control systems to reduce congestion at sags: An evaluation based on microscopic traffic simulation. Transportation Research Part C: Emerging Technologies 102, 411-426.

Lammert, M.P., Duran, A., Diez, J., Burton, K., Nicholson, A., 2014. Effect of platooning on fuel consumption of class 8 vehicles over a range of speeds, following distances, and mass. SAE International Journal of Commercial Vehicles 7(2), 626-639.

Larsen, R., Rich, J., & Rasmussen, T. K., 2019. Hub-based truck platooning: Potentials and profitability. Transportation Research Part E: Logistics and Transportation Review, 127, 249-264.

Larson, J., Kammer, C., Liang, K.Y., Johansson, K.H., 2013. Coordinated route optimization for heavy-duty vehicle platoons, 16th International IEEE Conference on Intelligent Transportation Systems (ITSC 2013). IEEE, pp. 1196-1202.

Larson, J., Munson, T., Sokolov, V., 2016. Coordinated platoon routing in a metropolitan network, 2016 Proceedings of the Seventh SIAM Workshop on Combinatorial Scientific Computing. SIAM, pp. 73-82.

Larsson, E., Sennton, G., Larson, J., 2015. The vehicle platooning problem: Computational complexity and heuristics. Transportation Research Part C: Emerging Technologies 60, 258-277.

Lee, W. J., Kwag, S. I., Ko, Y. D., 2021. The optimal eco-friendly platoon formation strategy for a heterogeneous fleet of vehicles. Transportation Research Part D: Transport and Environment, 90: 102664.

Li, S.E., Li, R., Wang, J., Hu, X., Cheng, B., Li, K., 2016. Stabilizing periodic control of automated vehicle platoon with minimized fuel consumption. IEEE Transactions on Transportation Electrification 3(1), 259-271.

Lu, X.Y., Shladover, S.E., 2011. Automated truck platoon control. California PATH Program Institute of Transportation Studies University of California, Berkeley.(remove)

Lu, X.Y., Shladover, S.E., 2014. Automated truck platoon control and field test. *Road Vehicle Automation*. Springer, 247-261.

Luo, F., Larson, J., 2021. A repeated route-then-schedule approach to coordinated vehicle platooning: Algorithms, valid inequalities and computation. Operations Research. https://doi.org/10.1287/opre.2021.2126.

Luo, F., Larson, J., Munson, T., 2018. Coordinated platooning with multiple speeds. Transportation Research Part C: Emerging Technologies 90, 213-225.

Mahdinia, I., Arvin, R., Khattak, A.J., Ghiasi, A., 2020. Safety, energy, and emissions impacts of adaptive cruise control and cooperative adaptive cruise control. Transportation Research Record 2674(6), 253–267.

Michaelian, M., Browand, F., 2000. Field experiments demonstrate fuel savings for close following. California PATH Research Report UCB-ITS-PRR-2000-14, 1-25.

Nourmohammadzadeh, A., Hartmann, S., 2016. The fuel-efficient platooning of heavy duty vehicles by mathematical programming and genetic algorithm. International Conference on Theory and Practice of Natural Computing. Springer, pp. 46-57.

Sokolov, V., Larson, J., Munson, T., Auld, J., Karbowski, D., 2017. Maximization of platoon formation through centralized routing and departure time coordination. Transportation Research Record 2667(1), 10-16.

Stehbeck, F., 2019. Designing and Scheduling Cost-Efficient Tours by Using the Concept of Truck Platooning. Junior Management Science 4(4), 566-634.

Sun, X., Yin, Y., 2019. Behaviorally stable vehicle platooning for energy savings. Transportation Research Part C: Emerging Technologies 99, 37-52.

Sun, X., Yin, Y., 2020. An auction mechanism for platoon leader determination in single-brand cooperative vehicle platooning. Economics of Transportation 28, 100233.

Sun, X., Yin, Y., 2021. Decentralized game-theoretical approaches for behaviorally-stable and efficient vehicle platooning. Transportation Research Part B: Methodological 153, 45-69.

Taylor, A., Droege, M., Shaver, G., Sandoval, J., Erlien, S., and Kuszmaul, J., 2020. Capturing the impact of speed, grade, and traffic on class 8 truck platooning. IEEE Transactions on Vehicular Technology, 69(10), 10506-10518.

Tsugawa, S., Jeschke, S., Shladover, S.E., 2016. A review of truck platooning projects for energy savings. IEEE Transactions on Intelligent Vehicles 1(1), 68-77.

Van De Hoef, S., Johansson, K.H., Dimarogonas, D.V., 2015. Fuel-optimal centralized coordination of truck platooning based on shortest paths, 2015 American Control Conference. IEEE, 3740-3745.

Van De Hoef, S., Johansson, K.H., Dimarogonas, D.V., 2018. Fuel-efficient en route formation of truck platoons. IEEE Transactions on Intelligent Transportation Systems 19(1), 102-112.

Wang, C., Gong, S., Zhou, A., Li, T., Peeta, S., 2020. Cooperative adaptive cruise control for connected autonomous vehicles by factoring communication-related constraints. Transportation Research Part C: Emerging Technologies 113, 124-145.

Xiao, Y., Konak, A., 2016. The heterogeneous green vehicle routing and scheduling problem with time-varying traffic congestion. Transportation Research Part E: Logistics and Transportation Review 88, 146-166.

Xue, Z., Lin, H., & You, J., 2021. Local container drayage problem with truck platooning mode. Transportation Research Part E: Logistics and Transportation Review, 147, 102211.

Yan, X.Y., Xu, M., Xie, C., 2022. Local container drayage problem with improved truck platooning operations.

You, J., Miao, L., Zhang, C., & Xue, Z., 2020. A generic model for the local container drayage problem using the emerging truck platooning operation mode. Transportation Research Part B: Methodological, 133, 181-209.

Zhang, L., Chen, F., Ma, X., Pan, X., 2020. Fuel economy in truck platooning: A literature overview and directions for future research. Journal of Advanced Transportation 2020, 2604012.

Zhang, W., Jenelius, E., Ma, X., 2017. Freight transport platoon coordination and departure time scheduling under travel time uncertainty. Transportation Research Part E: Logistics and Transportation Review 98, 1-23.

Zheng, Y., Xu, M., Wu, S., Wang, S., 2022. A Hybrid Vehicle Platoon for Connected and Automated Vehicles: Formulation, Stability Analysis, and Applications. *arXiv preprint arXiv:2107.11030*.